IEEE Access
Multidisciplinary ⋮ Rapid Review ⋮ Open Access Journal

Received July 30, 2020, accepted August 16, 2020, date of publication August 21, 2020, date of current version September 1, 2020.

Digital Object Identifier 10.1109/ACCESS.2020.3018418

A Cable-Driven Exosuit for Upper Limb Flexion Based on Fibres Compliance

JOSÉ LUIS SAMPER-ESCUDERO[1], ANTONIO GIMÉNEZ-FERNANDEZ[2], (Member, IEEE), MIGUEL ÁNGEL SÁNCHEZ-URÁN[1], AND MANUEL FERRE[1], (Member, IEEE)

[1]Centro de Automática y Robótica UPM-CSIC, Universidad Politécnica de Madrid, 28006 Madrid, Spain
[2]Departamento de Ingeniería, Universidad de Almería, 04120 Almería, Spain

Corresponding author: Manuel Ferre (m.ferre@upm.es)

This work was supported in part by the "Exoesqueleto Ligero para la Generación de Fuerzas en las Extremidades Superiores Aplicado a Tareas de Rehabilitación (ExoFlex)" Project funded by the Spanish Ministerio de Economía, Industria y Competitividad under Grant DPI-2015-68842-R, and in part by the "Lightweight Upper Limbs eXosuit for BImanual Task Enhancement/Exoesqueleto Ligero del Tren Superior para Ayuda a Tareas Bimanuales (LUXBIT)" funded by the Spanish Ministerio de Ciencia, Innovación y Universidades under Grant RTI2018-094346-BI00.

ABSTRACT Flexible soft exoskeletons, so-called exosuits, are robotic devices that interact with their users to assist or enhance muscle performance. Their lightweight design and lack of rigid parts allow assisting the user's natural motion without any constraints. They are thereby valuable in carrying out daily labour tasks and performing active stances of rehabilitation. Nonetheless, the usage of these devices in long-term applications demands anatomically adaptive designs and mechanisms to tackle textile artefacts and discrepancies in the human constitution. The soft exoskeleton described in this article is a textile-wearable design that assists shoulder and elbow flexion. The cable-driven actuation is embedded in a jacket by using several textiles and deformable parts. The inconveniences of using textile such as slipping, dampening, and pressure sores are tackled by combining textile layers with force-compliant sewing. The design also includes pieces for cable guidance, anchoring and support. These parts employ different tailoring methods so as to ease fabrication, wearing and cleaning. The motors and electronics, whose design is compatible with textiles too, are placed in a backpack. This configuration reduces forces from loads in motion and weight on the arm. Finally, the last part of the document discusses the preliminary results that have been obtained from four subjects who have worn the device.

INDEX TERMS Exosuit, flexible exoskeleton, soft exoskeleton, exoskeleton, upper limbs, human-robot interaction, textile, wearable, backpack.

I. INTRODUCTION

Exoskeletons' development has undeniably grown through the last decade, especially in lower limbs applications. The successful cases in gate-cycle restoration [1] and rehabilitation [2] have rocketed their irruption into different fields of society like labour assistance, entertainment, and telemanipulation, among others [3]. Early back in 2018, for example, Ford Automation announced the introduction of an exoskeleton in order to improve the working conditions in their assembling lines [4]. Similarly, Harvard has been studying different solutions for assisted walking and hiking during the last years [5], [6].

The associate editor coordinating the review of this manuscript and approving it for publication was Xiaoou Li.

Nowadays, the focus of research is on identifying the most compelling applications and mechanisms to move them into production. The reduction of the bulkiness and cost of these devices is a relevant matter in this regard; being two approaches principally applied to this end: rigid and soft exoskeletons.

Ongoing rigid devices are leaving behind bulky and heavy structures, seeking for lighter designs that are easier to wear [7]–[9]. However, they are still robot-like devices that interact with the wearers by embracing their anatomy [10] and rigidly connecting the articulations [11]. The most significant value of these devices lies in force application, either to mobilise and empower the wearer [12], [13]. The rigid structure of these robots supports the forces exerted to guide the user's limbs. Nonetheless, it also imposes mechanical

restrictions on the users' natural range of motion. This fact is not limiting when assisting repetitive motions (like human gate-cycle or elbow motion) but entails a drawback as the number of Degrees Of Freedom (DOF) increases [14]. Shoulder assistance is a proper example in this regard - this articulation has seven DOFs whose rotation axes are non-coincident. Additionally, the human body couples some of these degrees to perform daily living gestures [15]. Rigid designs deal with this complexity of the shoulder by constraining the articulation's workspace and adding passive joints [16]; thus, there is a trade-off between the users' mobility and bulkiness of the device [17], [18].

The counterpart of these rigid devices is soft exoskeletons. These so-called exosuits use soft mechanisms like Series-Elastic Actuators (SEA), cables, pneumatics and artificial muscles, among others, to transfer mobilisation forces to the wearer [19]–[22]. Therefore, there is a great interest in approaching new actuation, sensing and transparent control strategies. Proofs of such needs are, for example, the recent studies focused on the fabrics' actuation, textile-embeddable sensors' networks and soft human-robot interaction [23]–[25].

In this regard, note that there are recent pseudo-rigid designs that embed the device in textiles as well as make use of soft actuators [26], [27]. Their major difference to flexible devices lies in the functioning: flexible exoskeletons lack an entire structure that moves on its own. Instead, their actuation is supported on the anatomy of the wearer [28]. They are, therefore, not adequate to extend human capabilities but rather to assist them with moderated forces that the anatomy of the user can endure. Metabolic cost reduction and motion assistance are application cases where exosuits excel in [29], [30].

Such kind of tasks - like active rehabilitation, labour work and fatigue delay - are commonly related to long-term usage. As the wearing time increases, factors like the anchoring and coupling of the system to the human body raise their importance [31].

Coupling here alludes to how the exosuits transfers mobilising forces to the user. Coupling systems used in exoskeletons, either rigid and soft, tend to apply pressure to adjust the device to the user by using Velcro, straps and belts [32]–[34]. In short-term applications, such pressure-based fixation is not disturbing as long as its mean value does not surpass the vessel constrictions limits. However, in long-term usage, pressure can cause discomfort and other undesired effects like skin thinning [35], [36].

Moreover, the actuation of an exosuit also requires fixed points along the body, whereto support its functioning. The amount and fixation of these points are highly dependent on the mechanisms chosen. In cable-driven systems, for example, it is crucial to maintain the tension of the cable; whereas pneumatic-based systems should avoid variations of the conduits' section [37], [38]. Fulfilling such requirements is a challenging task in designing soft exoskeletons as they must deal with textile-related events like slippery of the fabrics, discrete perturbations from creases and seams, bad-fitting to the user anatomy and muscle volume changes during motion. Even though solutions on this regard lack consensus, there are three remarkable approaches for cable-driven systems: tangling cables around the body, force-compliant textile-design and study of the cable routing [39], [40].

Studies on lower limb exosuits have proven that tangling the actuation cables around the limbs prevents their lessening [41]. However, they can constrict the limb. A common solution is incorporating rigid surfaces or a fabric pattern that prevent such effect.

Fabric patterns are indeed a valuable asset in exosuit, given that the combination of textile layers can alter the behaviour of the cloth under forces. This modification can increase the adaption and fixation of the exoskeleton to the user, as seen in lower limbs designs [42].

Similarly, the routing of the cables can significantly affect actuation. Recent studies have demonstrated that there are parts of the human body that remain almost constant during motion. Therefore, cables routed through these paths are less sensitive to textile artefacts [43]. Generally, the placing of the cables also seeks to create a pulling motion that mobilises the member.

The portable exosuit presented in this article assists the upper limbs' flexion by using a new coupling system, based on textile fibres compliance. Other designs already use a base jacket or neoprene with Velcro or stiff webbing [40], [44]; however, they do not directly address the confection of the textile pattern to transfer forces to elbow and shoulder. The exoskeleton presented uses three types of breathable and thin fabrics whose characteristics promote comfort and force transference when stacked together. The usage of the jacket as base fabric along with a cable-anchoring method based on tailoring elements eases the wearing and dismantling of the exoskeleton.

The coupling developed transforms the pulling force from the cable in a pushing force over the anterior part of the limb. It avoids using rigid fixations and maintaining pressure with belts and straps. The rigid pieces over the arm have also been reduced either by using textile patterns and tailoring elements like button and rivets. The sewing pattern applied adapts the textile to the wearer's anatomy, delivering a fully-textile coupling that self-adjusts. Shoulder flexion uses two rigid pieces placed over the Trapezius as a pivot point. There is, in literature, an example whose functioning to elevate the shoulder recalls to the one presented here [45]. Nonetheless, we propose a user-adaptable design that can actuate the elbow and shoulder individually. Additionally, the design of our piece is such that it deforms during motion, enhancing, in such a manner, fitting to the user while protects the shoulder from Coaptation.

The outline of the document is as follows: the overall description of the exosuit is in Section II. This design adapts to different anatomies without constraining them by using a jacket with textiles layers stacked together — section III details how the fibres combine to increase the stiffness of

FIGURE 1. Exosuit to assist upper limbs flexion and backpack. This prototype uses an external power supply.

the cloth and mobilise the user. The design also includes two rigid pieces which improve shoulder actuation and protect the user. Section IV describes these pieces along with a backpack that the user can freely move around the workspace. The assistance capability of the device is assessed in Section V. This appraisal measures the surface electromyography signal (sEMG) of four healthy subjects while lifting a load. Finally, Section VI gathers the conclusions of this textile-based approach. Appendixes A and B describe the modelling of the system and the design methodology of the coupling, which can be adapted to different articulations.

II. DESCRIPTION OF THE EXOSUIT

The soft prototype in Fig. 1 can assist the elbow flexion wholly whereas it can only assist the shoulder partially up to 100 degrees. These motions can be combined to increase the workspace assisted. A commercial cycling jacket conforms the base cloth of the device. Several textile layers stack on this garment by using force-compliant sewing so as to improve adaption, fixation and force distribution. The jacket also contains three rigid pieces for shoulder actuation, force distribution and motors' fixation. Besides, the exosuit is portable by using the backpack in Fig. 1. The exosuit is inspired by tailoring methods to be washable and easy to dismantle.

The motors and electronics lie on the textile backpack. Currently, the power supply is a dc external source. The two motors are 24V@0.5A geared Maxon motors with torque exertion up to 5Nm. Two indexes have been applied in their selection: lightweight and easiness to modify the output range. These geared Maxon motors weigh 222gr each, accept a range of voltages from 24V to 48V and their form-shape is standardized allowing tuning their output by modifying the planetary gearbox without compromising the exosuit design.

The motors use a 5cm-pulley to deliver assistance forces up to 130N - which correspond to elevate fast the shoulder unloaded. The current configuration of motor torque and

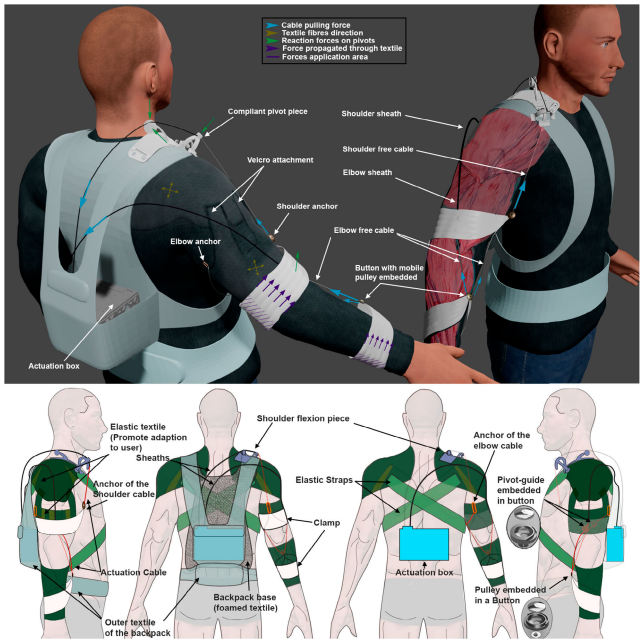

FIGURE 2. Overall description of the exosuit design. The forces considered in the design are marked as follows: blue denotes the cable pulling forces from fixations to motors; these forces provoke the reaction forces in green on the pivot and anchoring points. The pulling forces are transferred through the white clamps according to the purple arrows to the force application areas, in purple too. The extra textile layers are sewn, so their fibres match the yellow arrows.

pulley diameter deliver power enough to completely flex the shoulder up to 100 degrees in 2.3 seconds with a 2-kg load. The simulation of the exosuit, in Fig. 2, shows the two parts of this backpack: a modified baby carrier and a rigid box attachable to the garment with buttons and velcro. The commercial carrier selected is ergonomic for the back of the wearer, being certified for loads up to 20kg. An inner layer with foamed polymeric mesh has been added to the carrier to ease adjusting the actuation box. This foamed layer is sewn to the shoulder's harnesses but joins with velcro to the waistband. The harnesses of the backpack are embedded in the jacket to reduce their displacement.

The rigid Nylon-3d-printed box that contains the motors is attached to the outer and inner layers of the backpack by using buttons. A bolt goes through the pierced buttons to prevent their disassembling during actuation. The placement of the motors inside the box reduces the reaction forces applied to the user when two motions are combined. The electronics are in slots around them. This electronics consists of a board with conditioning and processing stages, an Nvidia Nano and a Texas Instrument processor board, as previously described in [46]. The total weight in the backpack is 890 gr. The backpack arrangement reduces the displacement of the centre of mass of the actuation; thus, fatigue and discomfort induced by carrying a mobile load are reduced too.

The system is cable-driven; therefore, the cables go from the motors, through the guidance pieces embedded in the jacket to the textile coupling with the user. The cables and their construction also play a relevant role in the actuation; in

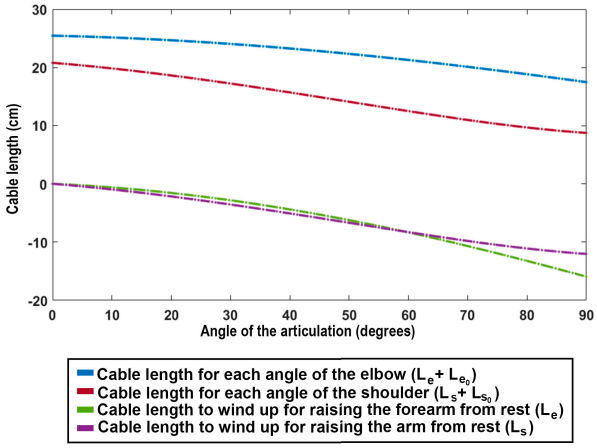

FIGURE 3. Cable lengths and retractions to obtain the desired flexion angle for each articulation of an individual. These values correspond to equations 1 to 9, using as bio-parameters: $L_a1 = 8.6$ cm, $L_a2 = 11.7$ cm, $L_f = 15.3$ cm, $w_f = 3.75$ cm, $w_p = 4.75$ cm, $h_p = 6.4$ cm. In the width of the arm we had to apply different values due to the anatomy of the user. In the elbow, L_e, we used half the sidearm-to-sidearm distance, being $wa = 4.35$ cm, whereas in L_s we took half the distance from biceps to triceps: $w_a = 5.05$ cm. The cylindrical assumption was equally applied in both equations but modifying the radius to the corresponding w_a. See Appendix A for formulation and symbols.

such a manner, the exosuit uses 0.68-mm Bowden steel cables consisting of 49 micro-steel threads weaved together in 7 ropes that conform the cable (tecni-cable ref 603.000.680). The cable has nylon coverage to avoid punctures and dismantling due to friction. We have specifically selected a cable with such construction to obtain reduced curvature radius and better resistance values (up to 500kg). The relation between the cable length and the articulation angle is in Fig. 3. These curves also display the cable retraction/extension needed to move each articulation from its rest position to the desired angle. See Appendix A for further detail about the theoretical modelling leading to them.

Additionally, we seize a snare-like anchoring with ferrules that safeguards the wearer by limiting the tensile strength of the assembling to 130 N, according to the manufacturer. Surpassing this value by any means provokes the sliding of the cable through the ferrule, dismantling the actuation. This construction prevents the rupture of the cable in sharp threads or lashes that could harm the user otherwise.

A steel-threaded tube with a rubber cover, just like the one in cycling transmissions, guides the cable from the motors to the lever point so as to maintain constant the length of the cable. This protection against abrasion is significantly stiff due to its 5cm-curvature-radius. Therefore, the cable housing is sensitive to shear forces and anatomical changes during muscle contractions. The routing of the cables reduces this effect by guiding them along the muscle fibres and tendon directions. Furthermore, the muscle bellies that suffer a grand volume change during contraction are bypassed by in-between muscles routing. The elbow routing uses this approach to evade the Biceps' volume change.

Nonetheless, there are still parts of the cables that need to retract and extend during actuation. For these areas with striking angulation and variable cable distances, we have designed a flexible housing that consists of a tube of polymeric mesh with thin rings inside. This housing can contract along with the cable but has a maximum retraction, given by the thickness of the rings. This configuration sets upper mechanical limits on the assistive motions.

As shown in Fig 2, the cable for shoulder flexion goes from the textile coupling with the user, at the distal arm, to a pivoting piece, described in Section IV, that displaces jointly with the Deltoids and Pectoralis. Similarly, the elbow cable goes over the forearm's Flexors and Brachioradialis, to the pivot point on the sidearm, beneath Biceps and Triceps. In this case, the cable uses the button in the textile coupling as a mobile pulley, see Sections III and IV, so as to balance the pulling forces during the pronosupination of the forearm. Specifically, the elbow cable anchors to the Triceps; from there, it goes to a pivot in the inner side of the arm. Then, it passes through the clamp bearing and replicates the trajectory to a pivot in the outer side of the arm.

In both cases, a rigid sheath guides the cables from the pivot to the motors. The motors are on the opposite side of the back. In such manner, the reaction forces are supported by the body; this avoids the slipping of the sheath out of the wearer's shoulder. Additionally, this collocation, along with a fixed length of the sheath, reduces the anchors to the user's back. It thereby promotes anatomy fitting while it prevents textile pulls and shear forces in the torso.

III. TEXTILE DESIGN FOR CABLE-DRIVEN INTERACTION

The exosuit presented seizes a lightweight and wearable design by combining three different textiles with force-compliant sewing. The textiles used are ProCool® Stretch-FIT Dri-QWick™ (appearing green or black in the figures), ProCool® Athletic Interlock Silver Fabric with SILVADUR™ (white textile in the images) and Snap Reinforcement Fabric (black mesh in the pictures). The cloth is hypo-allergenic, breathable and antimicrobial. The Dri-Qwick is soft, flexible and malleable, whereas the Interlock is rougher and only stretches in one direction. The Snap fabric is a thin polyester mesh commonly used as reinforcement in lightweight fabrics to improve their stiffness and firm.

In such manner, the exosuit uses Dri-Qwick as an adjustable base fabric by combining it with elastic Velcro; instead, the textile parts that transfer forces consist of two Interlock layers sewn together with a 45-degree rotation. The sewing of these layers also has to be force-compliant; otherwise, shear forces and creases will appear around the stitches. Three areas in the jacket have been enhanced thereof: the coupling zones (arm and forearm) and the Acromion's surroundings (Trapezius, Pectoralis and Teres Major), see Fig 4. These zones also count with patches of Snap reinforcement to distribute forces over a bigger surface and increase the stiffness of the fabric in the directions of the principal motion forces.

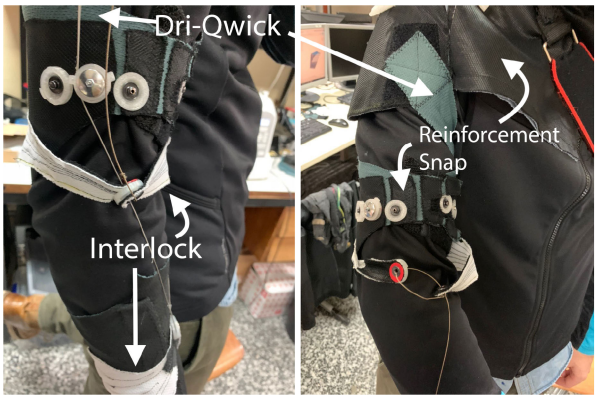

FIGURE 4. Textiles applied to couple the exosuit and to increase the stiffness of the shoulder pad. In some places, patches of Snap Reinforcement are combined with Dri-Qwick to limit the elasticity/deformation of the cloth.

FIGURE 5. Textiles used to interact with the user. The stitches coincide with the force direction of the pulling cable; thus, transfer forces to the Anterior part of the limb. B shows the layers of the shoulder armband and clamp, including the inner reinforcement patches; the metal ring over the Triceps whereto the elbow cable anchors is in c. The elbow cable, fixed to that metal ring, passes through the button-bearing in the elbow clamp balancing the pulling force, like shown in d. The elbow's pivot is in e, where the nylon coverage of the cable can also be seen. The pivot can be buttoned to three different positions what favours adaption to different arms' thicknesses.

Under this approach, our exosuit is majorly based on textiles, providing a coupling to the user that is less invasive than other solutions based on straps and rigid fastenings. Additionally, our design does not require compressing the limb to assure the fixation of the coupling. Instead, the fabric pattern self-adapts to the user anatomy when the exosuit applies a force. Such construction reduces wearing and maintenance times.

The coupling consists of a v-shaped clamp with two layers of Interlock cloth, see Fig 5. The fibres' directions in the cloth are crucial to obtain the desired deformation/stiffness of the fabric and a proper actuation. In this case, the Interlock layers, which only elongate in a single direction up to 10%, are stacked at 45°. Hence, their resulting direction converges to the direction of the primary mobilising force. The sewings are force compliant too, going from the cable anchoring to the posterior limb; there the clamp fixes to an elastic armband, made of Dri-QWick.

In consequence, the tightening of the cable, transferred through the stitches, pushes the clamp against the posterior part of the limb creating a levering force. There is an extra layer of Snap Reinforcement on the stitches and the posterior part of the clamp that increases stiffness. In consequence, the pulling force of the cable spreads through the resulting stiff cloth by the stitches.

The exosuit uses two of these clamps to interact with the user, one per assisted motion. Their design procedure, at Appendix B, is common to both of them except for the cable-to-textile mechanism. A pierced button joins the shoulder clamp extremes. The cable fastens throughout this button in a snare-like way. In contrast, the elbow clamp has a bearing disc, 3D-printed with Nylon, integrated into the button. The cable passes through the inner conduit formed when buttoned up, see Figs 5d and 2.

Each clamp is sewn to an elastic Dri-QWick armband whose fabric can elongate up to 40%. This armband lies beneath the jacket and the clamp with a twofold purpose: on the one hand, it prevents creases in the jacket that lead to discomfort and rub with the cables; on the other hand, it eases the fitting of the exosuit to different anatomies. In this context, the exosuit sizes (European M and L) tackle different anatomical lengths that would, otherwise, complicate fitting the rigid pieces in Section IV. In contrast, the armband is adaptable to different arm's thicknesses. Each clamp joins the armband and the jacket with a single straight stitch.

The pivot and cable anchors for the elbow lever are embedded in the shoulder armband. These pivots consist of a 3d-printed bearing disc that contains a fastening for the rigid sheaths. Their design allows riveting them to textiles by using high-duty 14-cm buttons, see Fig 5. High duty buttons have a fixation procedure based on a circular pattern of sharp teeth, so they do not tear the fabric. The bearing is buttoned to the pin that better fits the user's arm perimeter - there are three pins at each arm side. Moreover, a 4-mm bolt firmly fixes its position to prevent dismantling. The anchor of the elbow cable is a metal ring sewn to the posterior part of the armband, over the Medial Triceps Head. The lower part of the shackle coincides with the end of the Triceps Head, minimising the effect of muscle contraction in the cable.

The integration of these pieces into the armband exposes it to undesired frictions and forces. We have added 2-layer patches of reinforcement mesh to enhance friction resistance and stiffness while maintaining the elastic nature of the cloth. Additionally, the armband is fixed to a shoulder-pad by two elastic Velcro straps that twist around the arm. These details

appear in Figs 4 and 5b-e, along with the anchors and elbow pivots.

The shoulder-pad is a 2-layer-stack of reinforcement fabric sewn to the jacket to improve stiffness and fixation of the rigid pieces for shoulder actuation. It covers Acromial surroundings down to Pectoralis Major and Teres Major. A buckle over these muscles allows fastening an elastic strap around the torso that improves fitting. This belt is not compressive as it only reduces creases. The shoulder-pad also includes elastic zones in high movable areas like Pectoralis and Teres insertions.

IV. RIGID PIECES IN THE EXOSUIT

This section addresses those parts of the exosuit that endure and distribute high forces. These pieces merge with the textile design to complement it. All of them have been designed in Autodesk Fusion 360 and 3D-printed in Nylon. In some of them, Nylon thickness and filling pattern are crucial to reach a controlled deformation that improves anatomical adaption and force distribution during motion. Buttons and rivets apart, the exosuit uses three rigid pieces: a pivot for the shoulder, a support surface adaptable to the Trapezius and the actuation box.

The pivot is a rigid piece that increases the pulling angle of the cable and protects the articulation. The seven-degree kinematic chain of the shoulder is a highly movable part of the human body whose instantaneous rotation axis continually changes. Consequently, this delicate articulation has several singular configurations that expose thereof to external forces. One undesirable result of these forces is Coaptation, which defines the act of pushing the humerus straight into the shoulder socket. Such incidents are avoidable by placing the support point of the exosuit ahead of the articulation. Similarly, the controlled deformation of a piece can result in a better fitting to the movable surface of the shoulder; thus, prevent focused forces that overload the articulation.

The pivot, in Fig 6, considers these factors in its design; being three parts distinguishable in the piece: a fixation base at the back, a broad frontal base and a circular upper part whereto the sheath fastens. The back base is stiff as it is wherein the anchors to the jacket lie. The broad frontal base has a rounded bottom that eases its sliding over the jacket when a force is applied. Additionally, the centre of the piece is deformable; that allows upward and downward motion of the frontal base when a force is applied. Therefore, the reaction force from the cable displaces the frontal base, which improves fitting and distributes the force through the base.

This behaviour requires a proper initial placing of the piece in which all forces stand over the frontal base. To this end, there is a small curved protuberance between both bases. This piece collides with the Clavicle and Pectoralis Major muscle when it fits the user's anatomy, see the second image in Fig 6. The curvature between the back bases and the bulge derives from averaged measures of medical studies [47]–[49].

Nonetheless, the joint movement of the pivot piece with the Pectoral muscle exposes it to shear forces that also complicate

FIGURE 6. This piece acts as a pivot for the shoulder flexion. The base and deformation favours adaption during motion and distributes forces over the Pectoral. It is fixed to the wide base whose grooves favour fitting to the Trapezius. The left picture shows the deformation, in Autodesk Fusion 360, when a force of 90N is applied in the direction marked by the arrow. Maximum and minimum displacement is coloured from red to blue, respectively. The central and right images show the deformation and fitting of the piece when the shoulder performs a 90-degree flexion.

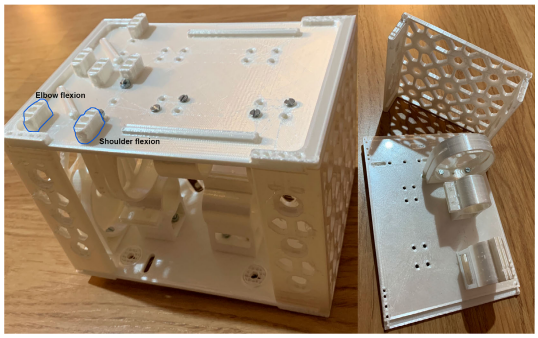

FIGURE 7. The motors are inside this box which can be embedded in the backpack with buttons at front and back. Walls materials have been optimized to reduce the weight. There are different conduits on the top to guide the sheaths and modify the reaction forces. In this prototype, they are fastened to the outer conduits, marked in blue. Each motor is supported by three pieces, displayed on the right: two anchor the motor and gearbox and a third one guides the cable and confines the pulley.

fixation to the body. The addition of lateral supports helps to mitigate the shear forces generated by the articulation's natural re-accommodation. These lateral stands also have a broad base so as to distribute the forces received. The latter issue - fixation - can be overcome by not fastening the pivot directly to the fabric; alternatively, it joints to the large piece over the Trapezius with a swivel. This joint assures the adequate placing of the pivot which complies with Pectoralis and Clavicle displacements.

The Trapezius motion and implication on shoulder movements make feasible fixing rigid large pieces. However, if the piece is broader than the muscle, forces in the Coronal Plane of the human body can provoke collision with the Deltoids and neck muscles, causing discomfort. Given the geometry of the muscle and complexion discrepancies between subjects, we have designed a flexible grooved base that adapts to the user-specific anatomy, as shown in Fig 6. The piece has hard parts without grooves that hold the fastens of the piece and sheaths' guidance elements.

The fixation of the piece is nonetheless prone to seams and creases, so it has a double anchoring. In essence, four buttons with bolts assure the relative placing of the piece to the Clavicle and shoulder, whereas two elastic belts surround its extremes to adapt the piece to the body. These straps anchor to buckles on the shoulder pad, fixing it too.

TABLE 1. Subjects information.

	Age	Gender	Height	Weight	R.Arm Per	C.Arm Per
1	25	M	187	83.5	28.8	32.3
2	27	M	179	68	26.6	29.1
3	31	F	170	72	27.2	31.9
4	28	M	168	74	31.5	37

* Units: Kilograms (kg) and centimetres (cm)
** R. Arm = Relaxed arm, non-contracted; Per = Perimeter
C. Arm = Contracted arm;
*** Perimeter measured at the middle line of the Biceps brachii.

The guidance element for the shoulder sheath is a pulley that directs the cable to the textile-embeddable box whereto the motors are fastened, see Fig. 7. Their placement, in opposition, mitigates the reaction forces when simultaneously assisting both motions. Additionally, they are perpendicular to the back so as to promote force transference to the harnesses of the backpack. The cable output position is also relevant in this regard. In this design, its placing generates an anti-clockwise reaction torque that extends the torso. The carrier backpack to which this box is attached has a medical ergonomic certification to bear efforts up to 20kg.

V. ASSISTANCE RESULTS AND DISCUSSION

The assistance capability of the exosuit has been assessed by analysing the muscle activity when the device is active. To this end, the Biceps and Deltoids sEMG signals of four informed subjects, in Table 1, have been measured with MyoWare sensors. These sEMG signals are only meant for evaluation, so they are not involved in the functioning of the device. The exosuit uses the feedback solely from encoders along with specific patterns of mechanical sensors, as described in Appendix A. The experiments, in accordance with the Universidad Politecnica de Madrid ethical rules, asked the participants (three males and one female) to wear the exosuit and perform five flexions of elbow and shoulder, with and without assistance from the device, both up to 90 degrees. The trajectory asked to perform was as follow: elevate and descend the limb in ten seconds, holding the upper and lower position of the gesture for two seconds.

A screen displayed the gesture to perform to the subjects, the timer and the trajectory performed in real-time. Eight markers were used with OptiTrack to track the arm's trajectory of the user during the whole experiment. The Biomech Tracking Protocol was applied in this regard: two markers at the back, one marker over the Acromion, three markers on the arm (two on the sidearm and one on the Triceps) and another two in the forearm.

After practising the gesture, the experiment started by performing the unassisted five repetitions. After resting for at least five minutes for muscle recovery, the exercise was repeated with assistance from the exosuit. Afterwards, the subjects had to wear a 0.75-kg wristband and repeat the whole experiment so as to evaluate assistance when mobilising loads.

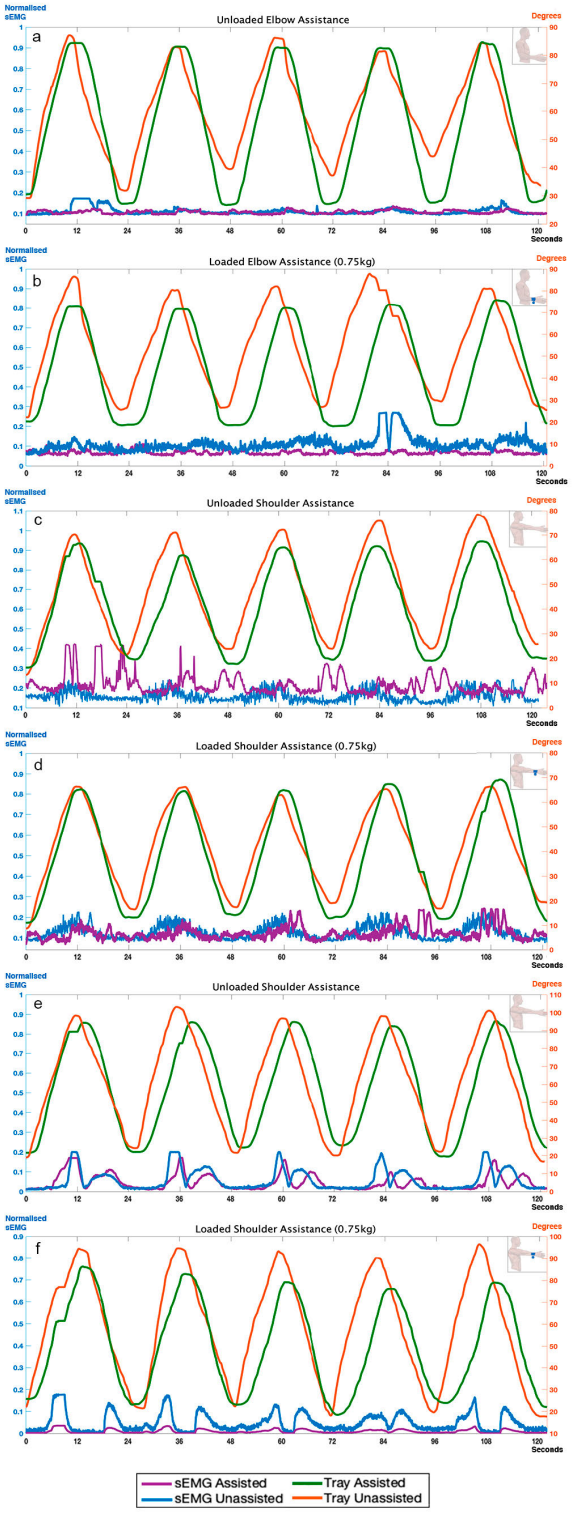

FIGURE 8. Assistance graphs from the experiment. First four graphs are from the same participant and the other two from a different subject. Each graph shows the trajectory and sEMG signal of the assisted and unassisted case. The sEMG signals are from the Biceps and Deltoids muscles, for the elbow and shoulder cases, respectively. The cases displayed are: a, elbow flexion without load; b, elbow flexion while carrying a 0.75-kg load; c,e shoulder flexion without load; d,f shoulder flexion while carrying a 0.75-kg load.

TABLE 2. Averaged experimental results for the elbow flexion.

Gesture performed	*Av. sEMG*	*sEMG std*	*sEMG Max*	*Flexion Ang*	*Flexion Ang. var*	*Rest Ang*	*Rest Ang. var*	*Hold (secs)*
Assisted elbow	0.071	0.012	0.122	87.195º	0.879	14.942º	3.298	1.15
Unassisted elbow	0.074	0.024	0.178	86.467º	13.793	18.985º	6.727	2.35
Assisted elbow with load[c]	0.073	0.018	0.159	73.038º	3.261	7.901º	0.505	1.32
Unassisted elbow with load[c]	0.099	0.034	0.269	82.038º	9.664	17.078º	5.80	2.27

[I] sEMG values are normalised with the maximum value measured for each subject.
[II] Ang = Angle, Av = Averaged, std = standard deviation, sEMG max = peak value reached in sEMG, var = variance, Rest Angle = initial/starting angle, Flexion Angle = Maximum angle reached by the user.
[III] The angle shown is the averaged metric of the angle results obtained for each subject.
[IV] Hold = Mean time that the subject hold the upper flexion position before extending the arm.

TABLE 3. Averaged experimental results for the shoulder flexion.

Gesture performed	*Av. sEMG*	*sEMG std*	*sEMG Max*	*Flexion Ang*	*Flexion Ang. var*	*Rest Ang*	*Rest Ang. var*	*Hold (secs)*
Assisted shoulder	0.133	0.027	0.253	69.588º	2.870	2.978º	1.358	0.71
Unassisted shoulder	0.113	0.025	0.203	76.780º	7.602	5.409º	7.754	1.29
Assisted shoulder with load[c]	0.104	0.025	0.226	63.450º	7.709	0.720º	2.339	0.77
Unassisted shoulder with load[c]	0.103	0.026	0.216	73.380º	5.599	3.624º	6.1604	1.56

[I] sEMG values are normalised with the maximum value measured for each subject.
[II] Ang = Angle, Av = Averaged, std = standard deviation, sEMG max = peak value reached in sEMG, var = variance, Rest Angle = initial/starting angle, Flexion Angle = Maximum angle reached by the user.
[III] The angle shown is the averaged metric of the angle results obtained for each subject.
[IV] Hold (secs) = Mean time that the subject hold the upper flexion position before extending the arm.

The processing of the data consisted of normalising the sEMG signals and removing the outliers. To this end, the sEMG from holding the wristband at 90-degree flexion during ten seconds was recorded before the experiments, for each subject and gesture. Then, a cubic spline interpolation was applied to translate Optitrack's trajectories to the sEMG timestamp. This off-line processing was carried in Matlab.

Table 2 gathers the average results obtained for elbow assistance. According to them, the soft exosuit effectively assists the elbow flexion by reducing its mean activation in a 5.5% and 26.36% in unloaded and loaded case, respectively. The device is also capable of delaying muscle fatigue and enhancing gesture repeatability even in the most natural case when the user is not carrying weight. In such a manner, the active exosuit reduces the variance of the maximum angle reached in a 64.84% and 93.19%, as well as the maximum flexion decay and peaks in muscle activation, as shown in Fig 9. Fig. 8 illustrates another relevant aspect in this regard: the starting angle differs between subjects but maintains through the whole experiment. These discrepancies between users are related to their natural anatomical pose; hence, the exosuit does allow the natural motion of the arm.

Such compliant actuation also delivers to the wearer capability to early stop the extension stage, as the assisted trajectory in Fig 8 reveals. In the graph, the impact of fatigue provokes a higher variance in the unassisted resting position. This effect is palliated by the exosuit, even though some variance still occurs. The trajectory results also reveal a fault in the actuation when the inertia increases: the loaded assisted cases reach a lower flexion of the elbow; this denotes cable friction or a textile perturbance directly related to the torque exerted. Despite that, subjects were still able to hold the upper position for significantly more time when the exosuit was active.

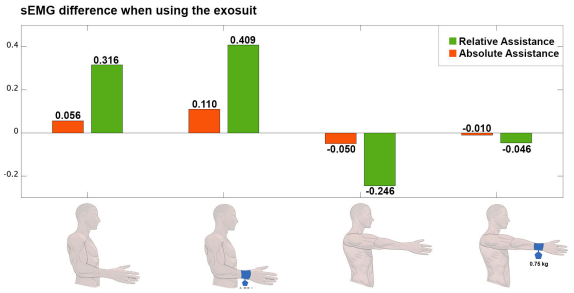

FIGURE 9. Averaged relative and absolute differences of the max sEMG signal measured. The value ranges from 0 to 1, corresponding 1 to maximum muscle contraction. A positive value indicates the benefit in sEMG achieved by the exosuit, whereas a negative value indicates that the exosuits increases fatigue. The four cases are from left to right: unloaded elbow flexion, loaded elbow flexion, unloaded shoulder flexion, loaded shoulder flexion.

The holding phase in a position where the forearm provokes high inertia is a demanding task that quickly increases muscle activation. The values on the column "Hold", along with the graphs, show that participants tended to short this phase when they were unassisted. There is also another remarkable aspect in these values: the assisted cases go beyond the expected two seconds. This fact is positive as it proves that the exosuit is efficient to reduce fatigue but also provide further basis for the existence of frictions.

These perturbations are a worrying issue as they reduce the torque delivered to the user, which eventually leads to under-assistance. Shoulder results are a clear example of such an undesired event. The assistance of the loaded shoulder, in Table 3, has a significant variance when reaching the maximum flexion, even surpassing the unassisted human variance. Furthermore, the average maximum angle reached with the active exosuit is lower too. The loaded assisted cases in Fig. 8d and 8f exhibit displacements of the trajectory

during motion, from 50 degrees on ahead. This fault in trajectory accomplishment is directly related to shoulder actuation. The sEMG signal and holding times provide further insight in this regard.

The first notable aspect of shoulder sEMG is that muscle activation increases when assisting the shoulder. However, the peaks of the shoulder graphs reveal that the participants maintained the upper position for less time without assistance. Specifically, according to the last column of Table 3, users could not maintain the upper position even for a second, on average, when the exosuit was not active. In contrast, they surpassed the second when the exosuit was active. This event explains the increase of the sEMG when assisting the shoulder. However, they could not remain in this position for two seconds. This fact, along with the trajectory deviation beyond 50 degrees, gives evidence of under-assistance.

Graphs 8e and 8f are illustrative in this regard. These charts are from a different subject which thoroughly relied on the exosuit to perform the motion. There, even though the repeatability is sufficient; the under-assistance is also manifest beyond 60 degrees. Another remarkable point from these results is that the subject's sEMG reduces as the weight increases. Therefore, the trust of the user in the exosuit to lead the motion grew as the weight did too.

To conclude, under-assistance can be corrected by increasing the motor torque. Nonetheless, applying a friction-optimization procedure can also solve the issue without increasing the weight of the system. These analysis and improvements of the device are prospect developments to carry out.

VI. CONCLUSION

The proposed exosuit can assist the upper limbs flexion by using a design completely based on textiles, although some points are to be improved. This wearable solution is portable, being the motors and electronics embedded in an ergonomic backpack. Our design, whose modelling is in Appendix A, combines different layers of fabrics by using a force-compliant sewing pattern. The stitches transfer the pulling force of the cable to the posterior part of the limb, which creates a levering effect. The exosuit is anatomically adaptable because it uses a height-based sizing to reduce textile excess and seams. In terms of assistance, the device can reduce muscle activation up to 26.36% as well as contribute to alleviating signs of fatigue in trajectory accomplishment. For example, users who wore the exosuit were able to extend their time in an exhausting position like arm extension. The paper includes the assistance assessment that obtained these values. In this study, four participants wore the exosuit and performed a set of flexion gestures. Their sEMG signals from Biceps and Deltoids muscles were recorded to determine the exosuit impact in both cases, unloaded and loading a 0.75-kg weight.

According to the results, an appropriate combination of fabrics allows increasing cloth stiffness in the principal motion directions as well as reducing seams and shear forces. To this end, the sewing pattern must be compliant with the stiffness and force directions. The clamps designed under this approach have effectively transferred the pulling force from the cable to the user's limb without constricting the limb. Additionally, the sewing pattern can distribute forces over a wide and stiff surface of the arm and consequently favour comfort. The design of the clamps, in Appendix B, is methodical so that it can be applied to different articulations and parts of the human body. In this case, the same procedure has been followed to create the coupling for elbow and shoulder flexion. In our case, the cables anchor to the clamps and textiles by using a button-based approach. This method has proven effective in the experiments without displacements or reported discomfort. Additionally, this anchoring method eases wearing and dismantling the exosuit.

Textile friction and slipping are a worrying issue when working with textiles. In our case, the stacking and combination of fabrics are adequate to deal with them thereof. However, the results of the experiments have shown the presence of inertia-related frictions. These perturbances were depictable in elbow assistance but led to under assistance in the shoulder. Therefore, textile stacking and sewing can effectively provide stiffness; such is why adequate routing and fixation of the cables are required. Further optimization of the cable paths can improve shoulder assistance to match the results obtained for the elbow. This fault in the design is a cornerstone for prospect improvement.

The addition of rigid parts in order to complement the operation of an exosuit has also proven useful for cable guidance and protection for the user. The presented exosuit uses the shoulder pivot to distribute forces and protect the articulation from undesired forces, such as Coaptation. Depending on the size and placement of these parts, the incorporation of deformable zones in them can improve anatomy adaption.

In terms of application, the participants wore the exosuit for an hour without reporting discomfort or showing pressure-related events such as reddening in the skin or pressure marks. A textile coupling like the one presented does not constrict the limbs. Therefore, it is appropriate for long-term applications. The device is also adequate for repetitive tasks in which fatigue or distraction could be an issue since it improves trajectory accomplishment and repeatability. Workers who manipulate loads like the ones in sectors such as logistics and manual labour are potential targets for such kind of devices given that muscle activation reduction can improve their postural hygiene. Fatigue signs are one major cause of injuries and work absence in these jobs, which can be palliated by such kind of devices. Commonly, these workers move through the workspace by performing a variety of gestures with specific anatomy-alterations. Rigid devices can easily restrict these motions.

In contrast, textile devices, like the one presented, can adapt to the natural motion of the user comfortably. This fact, along with their lightweight, makes of flexible exosuits a valuable asset in places where high assistance forces are not

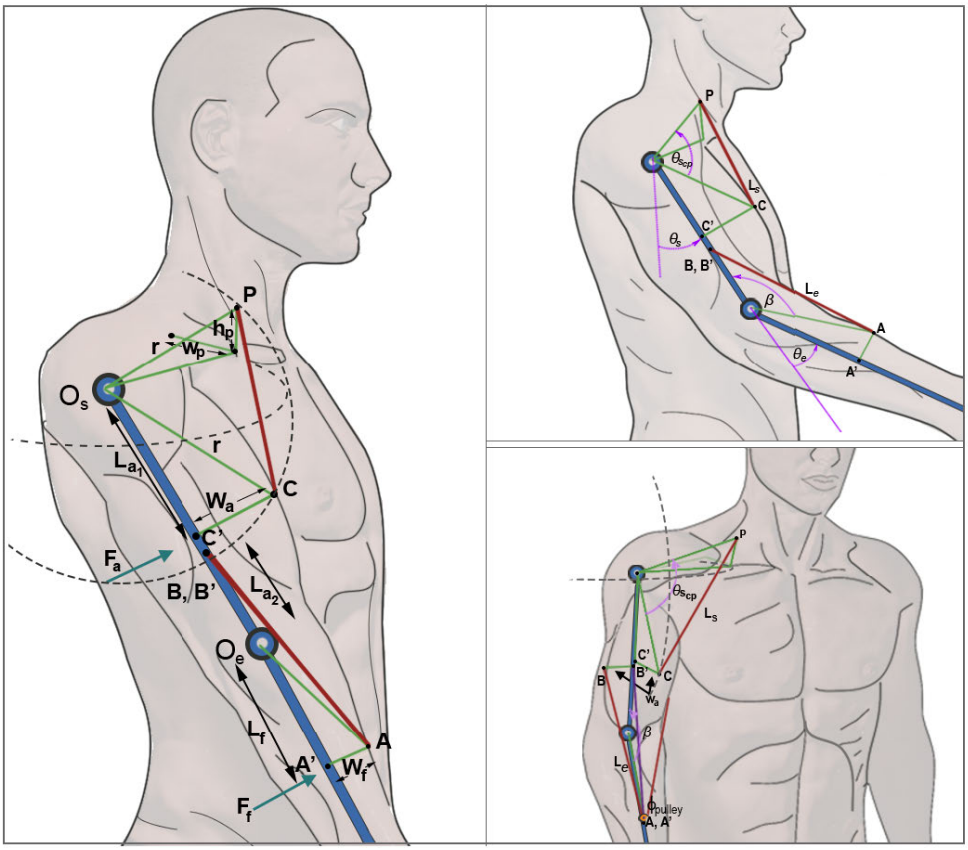

FIGURE 10. Forces and distances involved in the modelling of the cable extension and torque equations of the exosuit. The images on the right show the joint angles, reference points and lateral displacements that are not visible in the left view. Red lines indicate the position of the actuation cables, green lanes allude bio-mechanical triangles, and blue lines define the position of the bones and joints. B′ and C′ can be considered coincident but in the image have been distanced for clarity, so $L_a = L_{a_1} + L_{a_2}$. The definition of all the symbols is in Table 4.

required. Future work focuses on improving autonomy and assistance by optimising cable routing and frictions.

APPENDIX A
MODELLING OF THE EXOSUIT

This appendix describes the cable extension equations and relates them with the assistive and human torques for the device presented. Inelastic cable extension formulation from Murray *et al.* [50] has been extensively used in cable-driven exosuits to this end [51], [52]. Such formulation is not directly applicable in its original form to our design due to the routing discrepancies, which also demand specific formulation for each articulation. Our compliant design reinforces the assumptions of inelastic coupling and firm anchoring which have been previously accepted by other researchers [44]. Moreover, this formulation simplifies the mobilising forces of the clamps to a force vector applied on a point. The force application points for each motion correspond to Points A' and C' in Fig 10. These points are centred in the clamps. Additionally, the forearm and arm volumes under the clamps are modelled as cylinders of radius w_a, w_f, respectively. Table 4 describes all the symbols used in this regard.

In such a manner, the elbow extension equation can be derived from Murray's formulation by taking into account that the routing goes through the sidearm. Hence, the projection of the pivot point B (B') lies on the Humerus, whereas point A is over the forearm skin. Point A corresponds to the mobile pulley where the clamp anchors to the cable. Consequently, two triangles are to be solved ABO_e and $AA'O_e$. Obtaining $\overline{O_eA}$, by applying Pythagoras Theorem in the triangle $AA'O_e$, allows solving $\overline{AB}$ by using the Cosine Theorem.

Thus, the cable extension equation for the elbow is as follows:

$$l_e(\theta_e) = 2\left(\sqrt{\overline{AB'}^2 + w_a^2} + \phi_{pulley}\left(\frac{\pi}{3} - \frac{1}{2\cos\left(\arctan\left(\frac{w_a}{AB'}\right)\right)}\right)\right) - L_{e_0}; \quad \forall\theta_e > 0 \tag{1}$$

where:

$$\overline{AB'} = \sqrt{L_{a_2}^2 + w_f^2 + L_f^2 - 2L_{a_2}\cos\beta\sqrt{w_f^2 + L_f^2}} + \frac{\phi_{pulley}}{2} \tag{2}$$

$$\beta = \pi - \theta_e - \arctan\left(\frac{w_f}{L_f}\right) \tag{3}$$

TABLE 4. Equation symbols in Appendix A.

Symbol	Description
$L_e(\theta_e)$	Length of the elbow cable for a given flexion θ_e.
$L_s(\theta_s)$	Length of the shoulder cable for a given flexion θ_s.
θ_e	Angle of the elbow.
θ_s	Angle of the shoulder.
O_e	Center of the elbow articulation.
O_s	Virtual center of the spherical approximation of the shoulder articulation [53].
A	Point of the forearm clamp where the elbow cable pulls.
A'	Center point where clamp's forces apply in the forearm.
B	Pivot point for the elbow lever.
B'	Projection of the pivot point B into the humerus shaft.
C	Point of the arm clamp where the elbow cable pulls.
C'	Center point where clamp's forces apply in the arm.
P	Pivot point for the shoulder lever.
r	Radius of the shoulder's virtual sphere. $r = \sqrt{L_{a_1}^2 + w_a^2}$.
L_f	Distance from the elbow to the point of force application A'.
L_{a_1}	Distance from the shoulder center O_s to the point of force application C'.
L_{a_2}	Distance from the elbow to the pivot point over the humerus B'.
L_a	Arm length. Distances between B' and C' have been extended in the image for clarity. However, both points are assumed coincident given the design of the clamp. Then: $L_a = L_{a_1} + L_{a_2}$.
w_f	Half of the width of the forearm, from the bone to the forearm's surface in the middle-line of the clamp.
w_a	Half of the width of the arm, from the Humerus to the arm's surface in the middle-line of the arm's clamp.
w_p	Distance from the Coronal plane of the shoulder to the Clavicle. It also corresponds to half the horizontal distance from the Cavicle to the Trapezius backpart.
h_p	Height of the pivot piece for the shoulder. The piece deformation compensates the Clavicle displacement during motion.
ϕ_{pulley}	Diameter of the pulley embedded in a button of the forearm's clamp.
L_{s_0}	Shoulder's cable length when tighten at rest position. It can be approximated by the formula or directly measured on the user.
L_{e_0}	Elbow's cable length when tighten at rest position. It can be approximated by the formula or directly measured on the user.

In contrast, shoulder extension formulas must relate two points whose three-dimensional position varies due to the motion of the shoulder and the Clavicle. The position of the clamp and pivot piece allow applying spherical geometry to this case. In such a manner, there is a sphere of radius r that contains points C and D, whose centre is coincident with the shoulder's virtual one. Clinical and rehabilitation studies have demonstrated the convenience of this simplification when the shoulder intra-motion is not relevant [53], [54]. Additionally, we assume that the arm during the flexion of the shoulder does a lateral displacement equal to the width of the arm for a 90 degrees flexion. Then, the spherical distance between both points can be obtained by applying Napier and Delambre-Gauss half-angle Analogies with the Spherical Law of Haversines (denoted haversine here as $hav(\theta)$). The Haversines' Law is equivalent to the Spherical Cosine Theorem, but it has higher sensitivity to small variations of the angle. In consequence, the points C and P are defined using spherical geometry by their latitudes (φ_c, φ_p) and longitudes (λ_c, λ_p), in the shoulder virtual sphere.

$$hav(\theta_{s_{cp}}) = \cos\varphi_c \cos\varphi_p \sin\left(\frac{\lambda_p - \lambda_c}{2}\right)^2 + \sin\left(\frac{\varphi_p - \varphi_c}{2}\right)^2 \quad (4)$$

where:

$$\varphi_c = \arctan\left(\frac{w_a}{L_{a_1}}\right) + \theta_s - \frac{\pi}{2} \quad (5)$$

$$c\varphi_p = \arcsin\left(\frac{h_p}{\sqrt{w_a^2 + L_{a_1}^2}}\right) \quad (6)$$

$$c\lambda_c = \arctan\left(\frac{w_a}{L_{a_1}}\right)\sin\theta_s \quad (7)$$

$$c\lambda_p = \frac{\pi}{2} - \arcsin\left(\frac{w_p}{\sqrt{w_a^2 + L_{a_1}^2}}\right) \quad (8)$$

Applying the archaversine to this equation with Bessel formulation leads to define the extension equation for the shoulder that relates the joint angle of the user with the cable winding:

$$l_s(\theta_s) = 2\left(\sqrt{w_a^2 + L_{a_1}^2}\right)\sqrt{hav(\theta_{s_{cp}})} - L_{s_0} \quad (9)$$

Note that these equations are specific for each user. Thus, the first time the wearer uses the device, the distances of the arm, forearm and Clavicle-Trapezius have to be measured. This bio-information has to be updated if the user goes through significant anatomical changes. The solution of these equations for one individual has been displayed in Fig 3.

Finally, the cable length can be related with the tightening and assistive torque ($\tau_e = \frac{\partial l_c(\theta)}{\partial\theta} * f$, where f is the cable tension) to yield the dynamics expression by Euler-Lagrange:

$$\frac{\partial}{\partial t}\left(\frac{\partial\mathcal{L}}{\partial\dot{\theta}}\right) - \frac{\partial\mathcal{L}}{\partial\theta} = \tau_e + \tau_h - \beta\dot{\theta} = \frac{\partial l_c(\theta)}{\partial\theta} f + \tau_h - \beta\dot{\theta} \quad (10)$$

where:

$$\mathcal{L} = K(\theta, \dot{\theta}) + U(\theta) \quad (11)$$

$$\theta = [\theta_e, \theta_s] \quad (12)$$

$$lc = [l_s(\theta_s), l_e(\theta_e)], \quad (13)$$

where τ_h is the torque exerted by the human, $\mathcal{L}$ is the Lagrangian, β is a diagonal matrix with the viscous friction coefficients, whereas K and U respectively refer the Kinetic and Potential energies of the system:

$$K(\theta, \dot{\theta}) = \frac{1}{2}m_f\left(L_a^2\dot{\theta_s}^2 + L_f^2\dot{\theta_e}^2 + 2L_aL_f\dot{\theta_s}\dot{\theta_e}\cos(\theta_s - \theta_e)\right) + \frac{1}{2}m_a(L_a)^2\dot{\theta_s}^2 \quad (14)$$

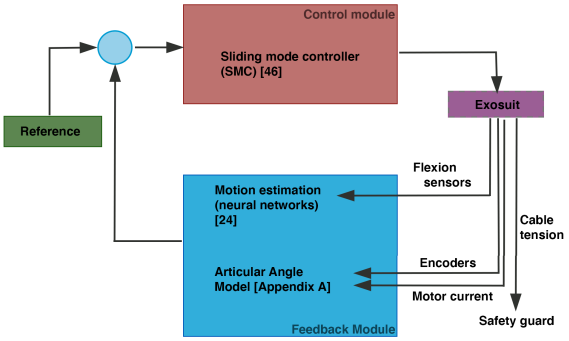

FIGURE 11. Scheme of the control loop of the exoskeleton during the experiments. Previous publications that explain each module are marked with []. The reference was specified in the graphic interface before the experiment.

$$U(\theta) = -(m_a + m_f)gL_a \cos\theta_s - m_f gL_f \cos\theta_e \qquad (15)$$

This modelling combined with a sliding mode controller and a wearable network of sensors has achieved adequate functioning and adaption to different users, further information about these systems and their functioning can be found in previous publications [24] and [46]. For the experiments, we have used a simpler version that does not use the cable tension but as a safety guard. In this case, the motor torque is obtained by measuring the current instead. Figure 11 shows the control loop.

APPENDIX B
DESIGN OF A COUPLING CLAMP

The coupling of an exoskeleton highly conditions usability and comfort on the user. In such a manner, we have designed a novel fully-textile coupling for exosuits that adapts to different articulations and members. A textile union like this is non-invasive for the user. It eludes long-term pressure and eases wearing and maintenance.

The clamp combines two layers of Interlock fabric at 45 degrees wherein the lane perpendicular to both fibres converges to the direction of the primary mobilising force. This principal direction is the projection of the lane from the support or pivot point to the posterior part of the member where forces apply.

The procedure to obtain the clamp pattern is as follows: an approximation of the relaxed arm shape is created in Autodesk Fusion 360 using medical studies for middle-aged adults [55], [56]. Then, a plane contained in the volume and perpendicular to the cable direction is intersected with the limb. The cable goes from the pivot point to the cable-anchoring point in the clamp. Our anchoring lies at the middle of the muscle, 1.5 cm ahead of the arm to prevent compression. A second plane delimits the clamp volume and determines its v-shape. To this end, the first plane is rotated 45 degrees around an axis at the cable-anchoring point, perpendicular to the cable. The perimeter area resulting from these operations delivers a tightly fitted clamp. Therefore, a lessened fitting is obtained by projecting the sidearm onto a tangential plane that contains the anchoring point.

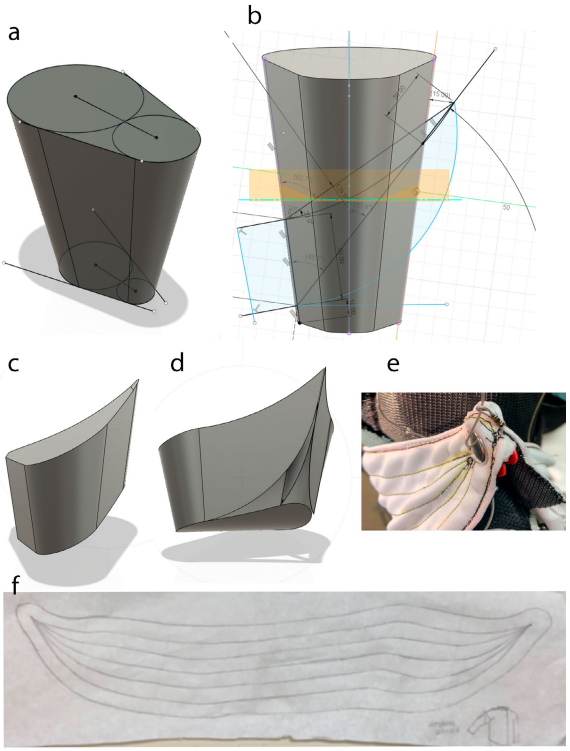

FIGURE 12. Methods to obtain the textile clamp for shoulder flexion, from CAD model to sewing pattern. a, member to actuate approximation; b, projection of the cutting lines in the middle plane; c, resulting volume of the clamp (fitted to the arm); d, clamp extension for loose-fitting; e, real clamp with button and snare-ferrule anchoring; f, sewing pattern obtained by unwrapping the CAD (with the sewing lines for force-transference and 1cm-padding included).

The unwrapping of the resulting geometry corresponds to the pattern sketch of the clamp. Figure 12 illustrates these steps in further detail.

REFERENCES

[1] A. Ganguly, D. Sanz-Merodio, G. Puyuelo, A. Goñi, E. Garces, and E. Garcia, "Wearable pediatric gait Exoskeleton–A feasibility study," in *Proc. IEEE/RSJ Int. Conf. Intell. Robots Syst. (IROS)*, Oct. 2018, pp. 4667–4672.

[2] C. Bayón, O. Ramírez, M. Velasco, J. I. Serrano, S. L. Lara, I. Martínez-Caballero, and E. Rocon, "Pilot study of a novel robotic platform for gait rehabilitation in children with cerebral palsy," in *Proc. 6th IEEE Int. Conf. Biomed. Robot. Biomechatron. (BioRob)*, Jun. 2016, pp. 882–887.

[3] S. J. Baltrusch, J. H. van Dieen, C. A. M. van Bennekom, and H. Houdijk, "Testing an exoskeleton that helps workers with low-back pain: Less discomfort with the passive SPEXOR trunk device," *IEEE Robot. Autom. Mag.*, vol. 27, no. 1, pp. 66–76, Mar. 2020.

[4] I. Pacifico, A. Scano, E. Guanziroli, M. Moise, L. Morelli, A. Chiavenna, D. Romo, S. Spada, G. Colombina, F. Molteni, F. Giovacchini, N. Vitiello, and S. Crea, "An experimental evaluation of the proto-MATE: A novel ergonomic upper-limb exoskeleton to reduce Workers' physical strain," *IEEE Robot. Autom. Mag.*, vol. 27, no. 1, pp. 54–65, Mar. 2020.

[5] A. T. Asbeck, S. M. M. De Rossi, I. Galiana, Y. Ding, and C. J. Walsh, "Stronger, smarter, softer: Next-generation wearable robots," *IEEE Robot. Autom. Mag.*, vol. 21, no. 4, pp. 22–33, Dec. 2014.

[6] F. A. Panizzolo, I. Galiana, A. T. Asbeck, C. Siviy, K. Schmidt, K. G. Holt, and C. J. Walsh, "A biologically-inspired multi-joint soft exosuit that can reduce the energy cost of loaded walking," *J. NeuroEng. Rehabil.*, vol. 13, no. 1, p. 43, Dec. 2016.

[7] G. S. Sawicki, O. N. Beck, I. Kang, and A. J. Young, "The exoskeleton expansion: Improving walking and running economy," *J. NeuroEng. Rehabil.*, vol. 17, no. 1, pp. 1–9, Dec. 2020.

[8] W. Huo, M. A. Alouane, Y. Amirat, and S. Mohammed, "Force control of SEA-based exoskeletons for multimode human–robot interactions," *IEEE Trans. Robot.*, vol. 36, no. 2, pp. 570–577, Apr. 2020.

[9] M. Monroy, M. Ferre, J. Barrio, V. Eslava, and I. Galiana, "Sensorized thimble for haptics applications," in *Proc. IEEE Int. Conf. Mechatronics*, Apr. 2009, pp. 1–6.

[10] D. Sanz-Merodio, G. Puyuelo, A. Ganguly, E. Garces, A. Goñi, and E. Garcia, "EXOtrainer project clinical evaluation of gait training with exoskeleton in children with spinal muscular atrophy," in *Advances in Robotics Research: From Lab to Market*. Cham, Switzerland: Springer, 2020, pp. 211–227.

[11] Y. Liu, S. Guo, H. Hirata, H. Ishihara, and T. Tamiya, "Development of a powered variable-stiffness exoskeleton device for elbow rehabilitation," *Biomed. Microdevices*, vol. 20, no. 3, p. 64, Sep. 2018.

[12] F. Lanotte, L. Grazi, B. Chen, N. Vitiello, and S. Crea, "A low-back exoskeleton can reduce the erector spinae muscles activity during freestyle symmetrical load lifting tasks," in *Proc. 7th IEEE Int. Conf. Biomed. Robot. Biomechatron. (Biorob)*, Aug. 2018, pp. 701–706.

[13] D. J. Hyun, H. Lim, S. Park, and S. Nam, "Singular wire-driven series elastic actuation with force control for a waist assistive exoskeleton, H-WEXv2," *IEEE/ASME Trans. Mechatronics*, vol. 25, no. 2, pp. 1026–1035, Apr. 2020.

[14] B. K. Dinh, M. Xiloyannis, C. W. Antuvan, L. Cappello, and L. Masia, "Hierarchical cascade controller for assistance modulation in a soft wearable arm exoskeleton," *IEEE Robot. Autom. Lett.*, vol. 2, no. 3, pp. 1786–1793, Jul. 2017.

[15] A.-M. Georgarakis, P. Wolf, and R. Riener, "Simplifying exosuits: Kinematic couplings in the upper extremity during daily living tasks," in *Proc. IEEE 16th Int. Conf. Rehabil. Robot. (ICORR)*, Jun. 2019, pp. 423–428.

[16] X. Li, Z. Jia, X. Cui, and L. Zhang, "Design, analysis and experiment of a non-humanoid arm exoskeleton for lifting load," in *Proc. IEEE Int. Conf. Intell. Robotic Control Eng. (IRCE)*, Aug. 2018, pp. 64–68.

[17] E. Trigili, S. Crea, M. Moisè, A. Baldoni, M. Cempini, G. Ercolini, D. Marconi, F. Posteraro, M. C. Carrozza, and N. Vitiello, "Design and experimental characterization of a shoulder-elbow exoskeleton with compliant joints for post-stroke rehabilitation," *IEEE/ASME Trans. Mechatronics*, vol. 24, no. 4, pp. 1485–1496, Aug. 2019.

[18] H.-C. Hsieh, D.-F. Chen, L. Chien, and C.-C. Lan, "Design of a parallel actuated exoskeleton for adaptive and safe robotic shoulder rehabilitation," *IEEE/ASME Trans. Mechatronics*, vol. 22, no. 5, pp. 2034–2045, Oct. 2017.

[19] S. Lessard, P. Pansodtee, A. Robbins, L. B. Baltaxe-Admony, J. M. Trombadore, M. Teodorescu, A. Agogino, and S. Kurniawan, "CRUX: A compliant robotic upper-extremity exosuit for lightweight, portable, multi-joint muscular augmentation," in *Proc. Int. Conf. Rehabil. Robot. (ICORR)*, Jul. 2017, pp. 1633–1638.

[20] L. Cappello, A. Pirrera, P. Weaver, and L. Masia, "A series elastic composite actuator for soft arm exosuits," in *Proc. IEEE Int. Conf. Rehabil. Robot. (ICORR)*, Aug. 2015, pp. 61–66.

[21] N. Thompson, A. Sinha, and G. Krishnan, "Characterizing architectures of soft pneumatic actuators for a cable-driven shoulder exoskeleton," in *Proc. Int. Conf. Robot. Autom. (ICRA)*, May 2019, pp. 570–576.

[22] C. M. Thalman, Q. P. Lam, P. H. Nguyen, S. Sridar, and P. Polygerinos, "A novel soft elbow exosuit to supplement bicep lifting capacity," in *Proc. IEEE/RSJ Int. Conf. Intell. Robots Syst. (IROS)*, Oct. 2018, pp. 6965–6971.

[23] R. J. Varghese, A. Nguyen, E. Burdet, G.-Z. Yang, and B. P. L. Lo, "Nonlinearity compensation in a multi-DoF shoulder sensing exosuit for real-time teleoperation," 2020, *arXiv:2002.09195*. [Online]. Available: http://arxiv.org/abs/2002.09195

[24] J. L. Samper-Escudero, A. F. Contreras-González, M. Ferre, M. A. Sánchez-Urán, and D. Pont-Esteban, "Efficient multiaxial shoulder-motion tracking based on flexible resistive sensors applied to exosuits," *Soft Robot.*, vol. 7, no. 3, pp. 370–385, Jun. 2020.

[25] B. W. K. Ang and C.-H. Yeow, "Design and modeling of a high force soft actuator for assisted elbow flexion," *IEEE Robot. Autom. Lett.*, vol. 5, no. 2, pp. 3731–3736, Apr. 2020.

[26] A. Ebrahimi, "Stuttgart exo-jacket: An exoskeleton for industrial upper body applications," in *Proc. 10th Int. Conf. Hum. Syst. Interact. (HSI)*, Jul. 2017, pp. 258–263.

[27] T. Chen, R. Casas, and P. S. Lum, "An elbow exoskeleton for upper limb rehabilitation with series elastic actuator and cable-driven differential," *IEEE Trans. Robot.*, vol. 35, no. 6, pp. 1464–1474, Dec. 2019.

[28] R. F. Natividad and C. H. Yeow, "Development of a soft robotic shoulder assistive device for shoulder abduction," in *Proc. 6th IEEE Int. Conf. Biomed. Robot. Biomechatron. (BioRob)*, Jun. 2016, pp. 989–993.

[29] A. T. Asbeck, K. Schmidt, I. Galiana, D. Wagner, and C. J. Walsh, "Multi-joint soft exosuit for gait assistance," in *Proc. IEEE Int. Conf. Robot. Autom. (ICRA)*, May 2015, pp. 6197–6204.

[30] F. A. Panizzolo, G. M. Freisinger, N. Karavas, A. M. Eckert-Erdheim, C. Siviy, A. Long, R. A. Zifchock, M. E. LaFiandra, and C. J. Walsh, "Metabolic cost adaptations during training with a soft exosuit assisting the hip joint," *Sci. Rep.*, vol. 9, no. 1, pp. 1–10, Dec. 2019.

[31] A. Rathore, M. Wilcox, D. Z. M. Ramirez, R. Loureiro, and T. Carlson, "Quantifying the human-robot interaction forces between a lower limb exoskeleton and healthy users," in *Proc. 38th Annu. Int. Conf. IEEE Eng. Med. Biol. Soc. (EMBC)*, Aug. 2016, pp. 586–589.

[32] D. J. Gonzalez and H. H. Asada, "Hybrid open-loop closed-loop control of coupled human–robot balance during assisted stance transition with extra robotic legs," *IEEE Robot. Autom. Lett.*, vol. 4, no. 2, pp. 1676–1683, Apr. 2019.

[33] D. Lee, E. C. Kwak, B. J. McLain, I. Kang, and A. J. Young, "Effects of assistance during early stance phase using a robotic knee orthosis on energetics, muscle activity, and joint mechanics during incline and decline walking," *IEEE Trans. Neural Syst. Rehabil. Eng.*, vol. 28, no. 4, pp. 914–923, Apr. 2020.

[34] Y. G. Kim, M. Xiloyannis, D. Accoto, and L. Masia, "Development of a soft exosuit for industrial applications," in *Proc. 7th IEEE Int. Conf. Biomed. Robot. Biomechatron. (Biorob)*, Aug. 2018, pp. 324–329.

[35] S. J. Bashir and A.-L. Chew, "Mechanical injury to the skin," in *Rook's Textbook Dermatology*, 9th ed. Oxford, U.K.: Wiley-Blackwell, 2016, pp. 1–37.

[36] A. F. T. Mak, M. Zhang, and E. W. C. Tam, "Biomechanics of pressure ulcer in body tissues interacting with external forces during locomotion," *Annu. Rev. Biomed. Eng.*, vol. 12, no. 1, pp. 29–53, Jul. 2010.

[37] M. Tschiersky, E. E. G. Hekman, D. M. Brouwer, J. L. Herder, and K. Suzumori, "A compact McKibben muscle based bending actuator for close-to-body application in assistive wearable robots," *IEEE Robot. Autom. Lett.*, vol. 5, no. 2, pp. 3042–3049, Apr. 2020.

[38] S. Lee, S. Crea, P. Malcolm, I. Galiana, A. Asbeck, and C. Walsh, "Controlling negative and positive power at the ankle with a soft exosuit," in *Proc. IEEE Int. Conf. Robot. Autom. (ICRA)*, May 2016, pp. 3509–3515.

[39] S. Zhao, Y. Yang, Y. Gao, Z. Zhang, T. Zheng, and Y. Zhu, "Development of a soft knee exosuit with twisted string actuators for stair climbing assistance," in *Proc. IEEE Int. Conf. Robot. Biomimetics (ROBIO)*, Dec. 2019, pp. 2541–2546.

[40] M. Xiloyannis, L. Cappello, B. K. Dinh, C. W. Antuvan, and L. Masia, "Design and preliminary testing of a soft exosuit for assisting elbow movements and hand grasping," in *Proc. 3rd Int. Conf. NeuroRehabilitation (ICNR)*, Segovia, Spain. Cham, Switzerland: Springer, Oct. 2016, pp. 557–561.

[41] Y. Ding, I. Galiana, A. T. Asbeck, S. M. M. De Rossi, J. Bae, T. R. T. Santos, V. L. de Araujo, S. Lee, K. G. Holt, and C. Walsh, "Biomechanical and physiological evaluation of multi-joint assistance with soft exosuits," *IEEE Trans. Neural Syst. Rehabil. Eng.*, vol. 25, no. 2, pp. 119–130, Feb. 2017.

[42] A. T. Asbeck, I. G. Bujanda, Y. Ding, R. J. Dyer, A. F. Larusson, B. T. Quinlivan, K. Schmidt, D. Wagner, C. Walsh, and M. Wehner, "Soft exosuit for assistance with human motion," U.S. Patent 10 427 293, Oct. 1, 2019.

[43] S. Lessard, P. Pansodtee, A. Robbins, J. M. Trombadore, S. Kurniawan, and M. Teodorescu, "A soft exosuit for flexible upper-extremity rehabilitation," *IEEE Trans. Neural Syst. Rehabil. Eng.*, vol. 26, no. 8, pp. 1604–1617, Aug. 2018.

[44] D. Chiaradia, M. Xiloyannis, C. W. Antuvan, A. Frisoli, and L. Masia, "Design and embedded control of a soft elbow exosuit," in *Proc. IEEE Int. Conf. Soft Robot. (RoboSoft)*, Apr. 2018, pp. 565–571.

[45] M. Hosseini, R. Meattini, A. San-Millan, G. Palli, C. Melchiorri, and J. Paik, "A sEMG-driven soft exosuit based on twisted string actuators for elbow assistive applications," *IEEE Robot. Autom. Lett.*, vol. 5, no. 3, pp. 4094–4101, Jul. 2020.

[46] D. Pont, A. F. Contreras, J. L. Samper, F. J. Sáez, M. Ferre, M. A. S. Sánchez, R. Ruiz, and A. García, "ExoFlex: An upper-limb cable-driven exosuit," in *Proc. 4th Iberian Robot. Conf.* Cham, Switzerland: Springer, 2020, pp. 417–428.

[47] C. E. Clauser, J. T. McConville, and J. W. Young, "Summary statistics and predictive equations," Antioch College, Yellow Springs, OH, USA, Tech. Rep., 1969.
[48] E. Berthonnaud, G. Herzberg, K. D. Zhao, K. N. An, and J. Dimnet, "Three-dimensional *in vivo* displacements of the shoulder complex from biplanar radiography," *Surgical Radiologic Anatomy*, vol. 27, no. 3, pp. 214–222, Aug. 2005.
[49] J. Andermahr, A. Jubel, A. Elsner, J. Johann, A. Prokop, K. E. Rehm, and J. Koebke, "Anatomy of the clavicle and the intramedullary nailing of midclavicular fractures," *Clin. Anatomy Off. J. Amer. Assoc. Clin. Anatomists Brit. Assoc. Clin. Anatomists*, vol. 20, no. 1, pp. 48–56, 2007.
[50] R. M. Murray, Z. Li, S. S. Sastry, and S. S. Sastry, *A Mathematical Introduction to Robotic Manipulation*. Boca Raton, FL, USA: CRC Press, 1994.
[51] M. Canesi, M. Xiloyannis, A. Ajoudani, A. Bicchi, and L. Masia, "Modular one-to-many clutchable actuator for a soft elbow exosuit," in *Proc. Int. Conf. Rehabil. Robot. (ICORR)*, Jul. 2017, pp. 1679–1685.
[52] C. J. Nycz, M. A. Delph, and G. S. Fischer, "Modeling and design of a tendon actuated soft robotic exoskeleton for hemiparetic upper limb rehabilitation," in *Proc. 37th Annu. Int. Conf. IEEE Eng. Med. Biol. Soc. (EMBC)*, Aug. 2015, pp. 3889–3892.
[53] R. Krishnan, N. Björsell, E. M. Gutierrez-Farewik, and C. Smith, "A survey of human shoulder functional kinematic representations," *Med. Biol. Eng. Comput.*, vol. 57, no. 2, pp. 339–367, Feb. 2019.
[54] W. Maurel and D. Thalmann, "Human shoulder modeling including scapulo-thoracic constraint and joint sinus cones," *Comput. Graph.*, vol. 24, no. 2, pp. 203–218, Apr. 2000.
[55] K. R. S. Holzbaur, W. M. Murray, G. E. Gold, and S. L. Delp, "Upper limb muscle volumes in adult subjects," *J. Biomechanics*, vol. 40, no. 4, pp. 742–749, Jan. 2007.
[56] E. B. Becker, "Measurement of mass distribution parameters of anatomical segments," *SAE Trans.*, vol. 81, no. 4, pp. 2818–2833, 1972.

JOSÉ LUIS SAMPER-ESCUDERO received the B.S. degree in industrial electronics and automation from the Universidad Politécnica de Cartagena, Murcia, Spain, in 2014, and the M.S. degree in automation and robotics from the Universidad Politécnica de Madrid, Spain, in 2016, where he is currently pursuing the Ph.D. degree in automation and robotics. In 2015, he was an Intern Engineer Trainee with the European Organization for Nuclear Research (CERN), Geneva, Switzerland. Since 2016, he has been a Research Engineer with the Centre for Automation and Robotics (CAR) UPM-CSIC. His current research interest includes soft actuation by using textiles and flexible exoskeletons.

ANTONIO GIMÉNEZ-FERNANDEZ (Member, IEEE) was born in Almería, Spain, in 1968. He received the M.S. degree in industrial engineering from the Polytechnic University of Madrid, in 1993, and the Ph.D. degree in industrial engineering from the University Carlos III of Madrid, Spain, in 2000.

From 1995 to 2006, he was an Associate Professor with the University Carlos III de Madrid and a member of the Robotics Lab, Research Group. Since 2006, he has been an Associate Professor with the University of Almería. He belongs to the Automation, Robotics and Mechatronics Group, University of Almería. He was involved in more than 20 national research and development projects (being the Main Researcher in four of them) and seven international projects, related to service robotics and processing automation (especially at the construction sector) and with machine design. He has written 26 international JCR articles, more than 50 conference papers, and four chapters at international books. His main research interests include mechanics and electronics of assistive robot, multibody modeling applied to mechanisms and vehicle, and teleoperated systems.

Dr. Giménez-Fernandez received the Extraordinary Doctorate Award from the University Carlos III of Madrid for his Ph.D.

MIGUEL ÁNGEL SÁNCHEZ-URÁN received the Laurea degree in control engineering and electronics and the Ph.D. degree (Hons.) in electronics from the Universidad Politécnica de Madrid (UPM), Madrid, Spain, in 1992 and 1998, respectively. From 1992 to 2001, he was with the Research Department, Telefónica, S.A. He is currently a Professor with the Department of Electrical and Electronic Engineering, Automatic Control, and Applied Physics, UPM, and a member of the Centre for Automation and Robotics UPM-CSIC. His research interests include automatic control and advanced telerobotics, haptics, test techniques, and signal processing. He is working on different projects and developments in these areas. He has been the author of several articles on human interfaces for teleoperation. He is also a member of the Study Committee SC-D1 (Materials and Emerging Test Techniques) of CIGRE.

MANUEL FERRE (Member, IEEE) received the Laurea degree in control engineering and electronics and the Ph.D. degree in automation and robotics from the Universidad Politécnica de Madrid (UPM), in 1992 and 1997, respectively. He worked as a Postdoctoral Researcher at the Human-Machine System Laboratory, Massachusetts Institute of Technology (MIT). He is currently a Full Professor with UPM. He has participated and coordinated several research projects in robotics and automatic control at national and international programs. His research interests include automatic control, advanced telerobotics, exoskeleton, and haptics. He has four patents of haptic devices and stereoscopic video cameras. He is the author of more than 150 publications and an Editor of the Springer Series on Touch and Haptic System. He is a member of the EuroHaptics Society, euRobotics, and CEA. He has served as the Chair of several committees of national and international societies.